Inverse estimation of parameters for multidomain flow models in soil columns with different macropore densities

Bhavna Arora,[1] Binayak P. Mohanty,[1] and Jennifer T. McGuire[2]

Received 20 April 2010; revised 8 February 2011; accepted 22 February 2011; published 19 April 2011.

[1] Soil and crop management practices have been found to modify soil structure and alter macropore densities. An ability to accurately determine soil hydraulic parameters and their variation with changes in macropore density is crucial for assessing potential contamination from agricultural chemicals. This study investigates the consequences of using consistent matrix and macropore parameters in simulating preferential flow and bromide transport in soil columns with different macropore densities (no macropore, single macropore, and multiple macropores). As used herein, the term "macropore density" is intended to refer to the number of macropores per unit area. A comparison between continuum-scale models including single-porosity model (SPM), mobile-immobile model (MIM), and dual-permeability model (DPM) that employed these parameters is also conducted. Domain-specific parameters are obtained from inverse modeling of homogeneous (no macropore) and central macropore columns in a deterministic framework and are validated using forward modeling of both low-density (3 macropores) and high-density (19 macropores) multiple-macropore columns. Results indicate that these inversely modeled parameters are successful in describing preferential flow but not tracer transport in both multiple-macropore columns. We believe that lateral exchange between matrix and macropore domains needs better accounting to efficiently simulate preferential transport in the case of dense, closely spaced macropores. Increasing model complexity from SPM to MIM to DPM also improved predictions of preferential flow in the multiple-macropore columns but not in the single-macropore column. This suggests that the use of a more complex model with resolved domain-specific parameters is recommended with an increase in macropore density to generate forecasts with higher accuracy.

Citation: Arora, B., B. P. Mohanty, and J. T. McGuire (2011), Inverse estimation of parameters for multidomain flow models in soil columns with different macropore densities, *Water Resour. Res.*, *47*, W04512, doi:10.1029/2010WR009451.

1. Introduction

[2] Containment of contaminants in the vadose zone is a viable option to prevent groundwater pollution from landfill and waste sites (Halton Waste Management Site, Canada, Yucca Mountain, Nevada, etc.). The feasibility of this option is generally hampered by the presence of macropores and fractures in the soil that can cause preferential transport of contaminants to groundwater [*National Research Council*, 1994; *Kladivko et al.*, 2001; *Böhlke*, 2002; *Jamieson et al.*, 2002]. Preferential flow modeling using the classical area-averaged Richards' equation is not enough to account for bypass flow through the macropores [*Beven and Germann*, 1982; *van Genuchten et al.*, 1990]. Additionally, early breakthrough and tailing due to preferential solute transport discredit the use of classical convection dispersion equation (CDE) [*Biggar and Nielsen*, 1962; *Liu et al.*, 1991; *Jury and Flühler*, 1992]. For a model to sufficiently reproduce characteristic features of preferential flow and transport, all sources of nonequilibrium should be effectively addressed [*Brusseau and Rao*, 1990]. For physical nonequilibrium processes, a common approach has been the use of continuum-scale models such as dual-porosity, dual-permeability, multiple-porosity or permeability models [*Gee et al.*, 1991; *Feyen et al.*, 1998; *Hendrickx and Flury*, 2001; *Šimůnek et al.*, 2003].

[3] The single-porosity model (SPM), the simplest conceptualization of the porous media, depends on a single-domain representation of the soil pore system. An equilibrium approach using SPM describes variably saturated water flow and solute transport through Richards' and convection dispersion equations, respectively. It has been used extensively in experimental studies to simulate transient conditions of porous media [e.g., *Šimůnek et al.*, 1999; *Jansson et al.*, 2005; *Köhne et al.*, 2006b]. Alternatively, two-domain conceptualization considers two interacting regions, one associated with the less permeable intra-aggregate pore region, or the rock matrix, and the other associated with the more permeable interaggregate, macropore, or fracture system. In this regard, mobile-immobile models (MIMs) consider water to be stagnant in the immobile domain [*van Genuchten and Wierenga*, 1976]. A widespread use of MIM has been reported by *Köhne et al.* [2009], especially for simulating preferential flow at

[1]Department of Biological and Agricultural Engineering, Texas A&M University, College Station, Texas, USA.
[2]Department of Geology and Geophysics, University of St. Thomas, St. Paul, Minnesota, USA.

0043-1397/11/2010WR009451

column and plot scales [cf. *Larsson et al.*, 1999; *Miller et al.*, 1999; *Abbasi et al.*, 2003; *Šimůnek et al.*, 2003]. Dual-permeability models (DPMs) assume both matrix and fracture continua to conduct fluids and solute [*Gerke and van Genuchten*, 1993; *Jarvis*, 1994]. Analogous to dual-porosity models, a number of approaches are available for DPMs which differ in the description of flow and solute transport in the preferential flow domain [*Germann*, 1985; *Ahuja and Hebson*, 1992; *Chen and Wagenet*, 1992] and of between-domain mass transfer [*Novák et al.*, 2000; *Köhne et al.*, 2004]. DPM has been applied at column, plot, and field scales [*Villholth and Jensen*, 1998; *Köhne and Mohanty*, 2005; *Dousset et al.*, 2007; *Köhne et al.*, 2009].

[4] A complete explicit representation of structural geometry and macroporosity in terms of well-defined physical parameters is usually not feasible with these continuum-scale models [*Vogel et al.*, 2000; *Gerke*, 2006]. In addition, farming practices and climatic patterns modify soil structure and change macropore density. Mechanized agricultural practices, rooting characteristics, biological activity, multiple cropping, etc., tend to disrupt the physical structure and cause changes to macroporosity at different times during a season [*Franzluebbers et al.*, 1995; *Schäffer et al.*, 2008]. Differences in macropore density are of particular concern for agricultural soils as leaching of chemicals through macropores can contribute to pollution from agricultural lands. Many investigators have shown that variation in pore size and connectivity, as a result of soil and crop management practices, affects the rate, flow, and retention of water [*Jarvis*, 2007]. Changes to model parameters reflecting an increase in the number or density of pores and its impact on preferential flow movement have not been addressed to date. The use of continuum-scale models to predict soil hydraulic properties and water movement requires adjustments to effective parameters to develop better agreement between observations and predictions. Previous studies have shown that soil hydraulic parameters need to be altered at both spatial and temporal scales to accurately reproduce preferential flow occurring through the macropores [*Logsdon and Jaynes*, 1996; *Das Gupta et al.*, 2006]. The focus of the present study is to test whether transport through macropores is a function of its density and if consistency in soil hydraulic parameters can be maintained while accounting for changes in macropore density.

[5] A problem of increasing model complexity (from SPM to MIM to DPM) is the task of understanding how these models compare under different scenarios. Continuum-scale models have resulted in different best model performances in the past on the basis of field or experimental settings being explored. For example, *Köhne et al.* [2006a] found a triple-porosity model (DPM in conjunction with MIM) to yield better results for tracer transport (Br^-), while the dual-permeability model performed better for adsorptive solutes (isoproturon and terbuthylazine) in a macroporous (aggregated) column. Nonetheless, both models behaved in a similar manner for an aggregated soil column with time-variant sorption. Evaluation and intercomparison of models can provide meaningful insights on the suitability of these models under different conditions (e.g., initial and boundary conditions or prominence versus lack of preferential flow). This study evaluates the performance of SPM, MIM, and DPM using designed soil column experiments with artificial macropores under conditions of different macropore densities and distributions (e.g., single (central) macropore, low-density (3 macropores), and high-density (19 macropores) columns). Model comparison, especially in multiple-macropore columns, offers a closer representation of the agricultural field. The specific objectives of this study are (1) to find the degree of model complexity (SPM, MIM, or DPM) that can adequately describe preferential flow in the single (central) as well as in low- and high-density multiple-macropore columns and (2) to evaluate if domain-specific parameters obtained from inverse modeling of homogeneous and single (central) macropore columns can consistently represent those individual domains in both low- and high-density multiple-macropore columns during transient flow and transport conditions. In summary, the evaluation of continuum-scale models and consideration of changes in macropore density are beneficial for quantifying contaminant transport, particularly through agricultural soils.

2. Continuum-Scale Models for Flow and Transport in Macroporous Soil

[6] Figure 1 depicts the characteristic features of continuum models (SPM, MIM, and DPM) for a hypothetical infiltration scenario of a central macropore column. In this study, matrix domain is chosen as the sole porous medium for flow in conceptualizing the single-porosity model. A unimodal pore size distribution is sufficient for describing the closed-form expressions for the hydraulic conductivity functions for the equilibrium SPM. The MIM approach represents the flow field through the macropore (mobile) domain and allows for water and solute transfer between the mobile and immobile regions. As opposed to SPM, the mobile-immobile model describes soil hydraulic functions using the macropore (mobile) domain parameters and utilizes information on matrix (immobile) domain for quantifying the inter-domain mass transfer. The DPM approach uses two different hydraulic functions, one for each domain, for describing flow through the column. Exchange between the matrix and macropore domains is established through a first- or second-order coupling term. A summary of the continuum scale flow and transport models is given in sections 2.1–2.3.

2.1. Single-Porosity Model

[7] In the one-dimensional single-porosity model, Richards' equation (equation (1)) is used for describing variably saturated flow and CDE (equation (2)) for modeling solute transport:

$$\frac{\partial \theta}{\partial t} = \frac{\partial}{\partial z}\left[K(h)\left(\frac{\partial h}{\partial z} + 1\right)\right] - S \tag{1}$$

$$\frac{\partial \theta c}{\partial t} + \frac{\partial \rho s}{\partial t} = \frac{\partial}{\partial z}\left(\theta D \frac{\partial c}{\partial z}\right) - \frac{\partial qc}{\partial z} - \mu(\theta + \rho s) + \gamma\theta + \gamma\rho, \tag{2}$$

where t is time [T]; z is the vertical coordinate positive upward [L]; θ is the water content [$L^3\ L^{-3}$]; h is the pressure head [L]; K is the unsaturated hydraulic conductivity [$L\ T^{-1}$]; S is a sink term; c and s are solute concentrations in the liquid [$M\,L^{-3}$] and solid phases [$M\,M^{-1}$], respectively; ρ is the soil bulk density [$M\ L^{-3}$]; q is the volumetric flux density [$L\ T^{-1}$]; μ is a first-order rate constant [T^{-1}]; γ is a zero-order rate constant [$M\,L^{-3}\,\mathrm{T}^{-1}$]; and D is the dispersion coefficient [$L^2\ T^{-1}$]. This

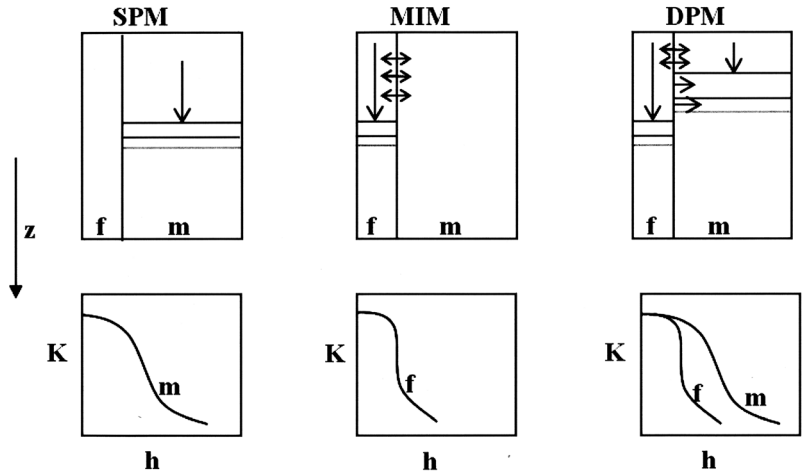

Figure 1. Schematic representation of the single-porosity model (SPM), mobile-immobile model (MIM), and dual-permeability model (DPM) along with their corresponding water retention characteristic curves. Symbols: z, depth coordinate; f, fracture or macropore or mobile domain; m, matrix or immobile domain; K, hydraulic conductivity; h, pressure head.

formulation allows a single-porosity model to describe flow and transport that is uniform and at local equilibrium [*Šimůnek et al.*, 2003; *Köhne et al.*, 2009].

2.2. Mobile-Immobile Model

[8] Richards' equation is used to simulate mobile water, and a source-sink term is used to account for water exchange with the soil matrix (immobile region) [*Šimůnek et al.*, 2001; *Köhne et al.*, 2006a]:

$$\frac{\partial \theta_m}{\partial t} = \frac{\partial}{\partial z}\left[K(h_m)\left(\frac{\partial h_m}{\partial z} + 1\right)\right] - \Gamma_w^{\mathrm{MIM}} \tag{3}$$

$$\frac{\partial \theta_{im}}{\partial t} = \Gamma_w^{\mathrm{MIM}} = w\left(Se^m - Se^{im}\right), \tag{4}$$

where Γ_w^{MIM} is the water transfer rate from the mobile to immobile region [T^{-1}], w is a first-order rate coefficient [T^{-1}], and Se^m and Se^{im} are effective fluid saturations in the mobile and immobile regions, respectively. Convective-dispersive solute transport is assumed for the mobile region and is analogous to water flow. A first-order solute exchange process is employed between the two regions [*Šimůnek et al.*, 2003]:

$$\frac{\partial \theta_m c_m}{\partial t} + \frac{\partial \rho_m s_m}{\partial t} = \frac{\partial}{\partial z}\left(\theta_m D_m \frac{\partial c_m}{\partial z}\right) - \frac{\partial q_m c_m}{\partial z} - \mu \theta_m c_m - \Gamma_s^{\mathrm{MIM}}, \tag{5}$$

$$\frac{\partial \theta_{im} c_{im}}{\partial t} + \frac{\partial \rho_{im} s_{im}}{\partial t} = -\mu \theta_{im} c_{im} + \Gamma_s^{\mathrm{MIM}}, \tag{6}$$

$$\Gamma_s^{\mathrm{MIM}} = w_s(c_m - c_{im}) + \Gamma_w^{\mathrm{MIM}} c^*, \tag{7}$$

where Γ_s^{MIM} is the solute transfer rate between the two regions [$M\ L^{-3}\ T^{-1}$], w_s is the constant first-order diffusive solute mass transfer coefficient [T^{-1}], and c^* is equal to c_m for $\Gamma_w^{\mathrm{MIM}} > 0$ and c_{im} for $\Gamma_w^{\mathrm{MIM}} < 0$.

2.3. Dual-Permeability Model

[9] In the dual permeability model, water flow in both macropore (subscript f) and matrix (subscript m) domains is described by two coupled Richards' equations [*Gerke and van Genuchten*, 1993]:

$$\frac{\partial \theta_f}{\partial t} = \frac{\partial}{\partial z}\left(K_f \frac{\partial h_f}{\partial z} + K_f\right) - \frac{\Gamma_w}{w_f} \tag{8}$$

$$\frac{\partial \theta_m}{\partial t} = \frac{\partial}{\partial z}\left(K_m \frac{\partial h_m}{\partial z} + K_m\right) - \frac{\Gamma_w}{1 - w_f}, \tag{9}$$

where w_f is the dimensionless volume factor defined as the ratio of the macropore domain volume (V_f) relative to the total soil volume (V_t):

$$w_f = \frac{V_f}{V_t}, \tag{10}$$

where Γ_w is the rate of water exchange between the two domains [T^{-1}] described with first-order mass transfer for DPM1 as

$$\Gamma_w^{\mathrm{DPM1}} = \alpha_w\left(h_f - h_m\right), \tag{11}$$

in which α_w is a first-order mass transfer coefficient for water [$L^{-1}\ T^{-1}$] given by

$$\alpha_w = \frac{\beta}{a^2} K_a \gamma_w, \tag{12}$$

where β is a dimensionless geometry-dependent shape factor, a is the characteristic length of the aggregate [L] (i.e., radius of the cylindrical aggregate for the single-macropore column and half-width diffusion length between the macropores and the soil matrix for the multiple-macropore columns), K_a is the hydraulic conductivity of the fracture-matrix interface region [$L\ T^{-1}$], and γ_w is a dimensionless scaling factor. Since

fracture coatings were absent for artificial macropores in this study, K_a was evaluated as follows:

$$K_a = 0.5\left[K_f\left(h_f\right) + K_m(h_m)\right]; \tag{13}$$

DPM with a second-order term (DPM2) for interdomain mass transfer of water was also considered [*Köhne et al.*, 2004]:

$$\Gamma_w^{\mathrm{DPM2}} = \frac{\beta K_a}{2a^2}\frac{\left(h_f - h_m\right)\left(|h_m - h_i| - |h_f - h_i|\right)}{|h_m - h_i|}, \tag{14}$$

where h_i is the initial pressure head assumed to be equal for matrix and macropore [L]. For DPM2, K_a is evaluated as

$$K_a = \frac{pK_m(h_m) + K_m\left(h_f\right)}{p+1}, \tag{15}$$

where p is a weighting factor for which an average value of 17 was found to be suitable for a range of hydraulic properties and initial conditions [*Köhne et al.*, 2004]. For both DPM1 and DPM2, geometrical parameters can be derived according to *Gerke and van Genuchten* [1996] as

$$\beta = \frac{1}{\left[0.19\ln(16\zeta)\right]^2}, 1 < \zeta < 100 \tag{16}$$

with

$$\zeta = \frac{a+b}{b}, \tag{17}$$

where b is the radius of the cylindrical macropore [L].

[10] Transport of nonreactive solutes in DPM is described by two coupled convection-dispersion equations:

$$\frac{\partial}{\partial t}\left(\theta_f c_f\right) = \frac{\partial}{\partial z}\left(\theta_f D_f \frac{\partial c_f}{\partial z} - q_f c_f\right) + \frac{\Gamma_s^{\mathrm{DPM}}}{w_f} \tag{18}$$

$$\frac{\partial}{\partial t}\left(\theta_m c_m\right) = \frac{\partial}{\partial z}\left(\theta_m D_m \frac{\partial c_m}{\partial z} - q_m c_m\right) + \frac{\Gamma_s^{\mathrm{DPM}}}{1 - w_f}, \tag{19}$$

where Γ_s^{DPM} is the solute mass transfer term [T^{-1}] given by

$$\Gamma_s^{\mathrm{DPM}} = \alpha\left(1 - w_f\right)\left(c_f - c_m\right) + \begin{cases} \Gamma_w^{\mathrm{DPM}} c_f, \Gamma_w^{\mathrm{DPM}} \geq 0 \\ \Gamma_w^{\mathrm{DPM}} c_m, \Gamma_w^{\mathrm{DPM}} < 0, \end{cases} \tag{20}$$

in which α is a first-order solute transfer coefficient of the form

$$\alpha_s = \frac{\beta}{a^2} D_a(\theta), \tag{21}$$

in which D_a is an effective diffusion coefficient [$L^2\ T^{-1}$] that is obtained analogous to K_a (equation (13)).

3. Experimental Setup

3.1. Multiple-Macropore Columns

[11] Soil column setup used in this study has been described in detail elsewhere [*Castiglione et al.*, 2003]. Only salient features of the setup are mentioned here. Two soil columns 75 cm long and 24 cm wide were constructed with 3 and 19 vertical macropores in one half of the column cross section and soil matrix in the other half (Figure 2). Soil used in the experimental setups was sandy loam (Typic Haploxeralf) with a 6% clay fraction (mostly Kaolinite). Soil packing was done using a piston compactor to attain a dry bulk density of 1.56 g cm^{-3}. Hollow stainless steel tubes of 1 mm diameter were used to create the macropores in one half of the column cross section. Designed pores with cylindrical diameter of 1 mm were characterized as macropores [*Jarvis*, 2007]. Polyacrylamide, a water-soluble polymer, was used along the macropore walls to help stabilize the artificially created pores. At the bottom of the column, 15 cm high vertical dividers were installed to form six pie-shaped chambers (Figure 2). These were useful in maintaining separate outflow measurements from the two halves with and without macropores and also for regulating bottom boundary conditions of pressure head.

[12] Water and bromide concentrations were monitored using twelve time domain reflectometry (TDR) probes installed at 5, 15, 25, 35, 45, and 55 cm depths from the top of the column in both halves of the column cross section (Figure 2). Minitensiometers were used to register matric potential in the matrix domain. Tensiometers were placed 5 cm apart in the soil matrix, with the first tensiometer close to the top of the column (Figure 2). Horizontal heterogeneity in pressure potential was captured by two sets of (six) tensiometers placed around the circumference of the soil column at depths of 50 and 75 cm. These were useful in comparing pressure head profiles of the chambers with and without macropores. Analogous to these circumferential tensiometers, outflow rates and flux-averaged Br^- concentrations were measured separately for the six effluent chambers. A fraction collector was used intermittently to collect outflow from the bottom at small time intervals (5 min).

[13] Boundary conditions (pressure heads) at the top of the soil column were maintained using a tension infiltrometer with a matching diameter disc (24 cm). Bottom boundary conditions were suction pressure heads varying between 0 and 30 kPa.

3.2. Homogeneous and Central Macropore Columns

[14] Two laboratory soil columns were filled with the same sandy loam soil to create a homogeneous column and another column with a central macropore (Figure 3). The central macropore column was provided with a single macropore of 1 mm diameter. A hollow stainless steel tube of equivalent diameter (1 mm) was used for this purpose. Soil packing, installation of TDRs and tensiometers, and boundary condition monitoring were very similar to the multiple-macropore columns.

3.3. Flow and Transport Experiments

[15] Infiltration and drainage experiments were performed on all four experimental columns, the homogeneous soil, central macropore, and low-density (3) and high-density (19) multiple-macropore columns. For all infiltration experiments, variability in pressure head profiles was approximately between −210 cm at the top to −42 cm at the bottom of the column at the start of the experiment (Table 1). Observations at all 13 tensiometer locations in the soil were used to describe initial conditions at depth layers of 0–5, 5–10, 10–15, 15–20,

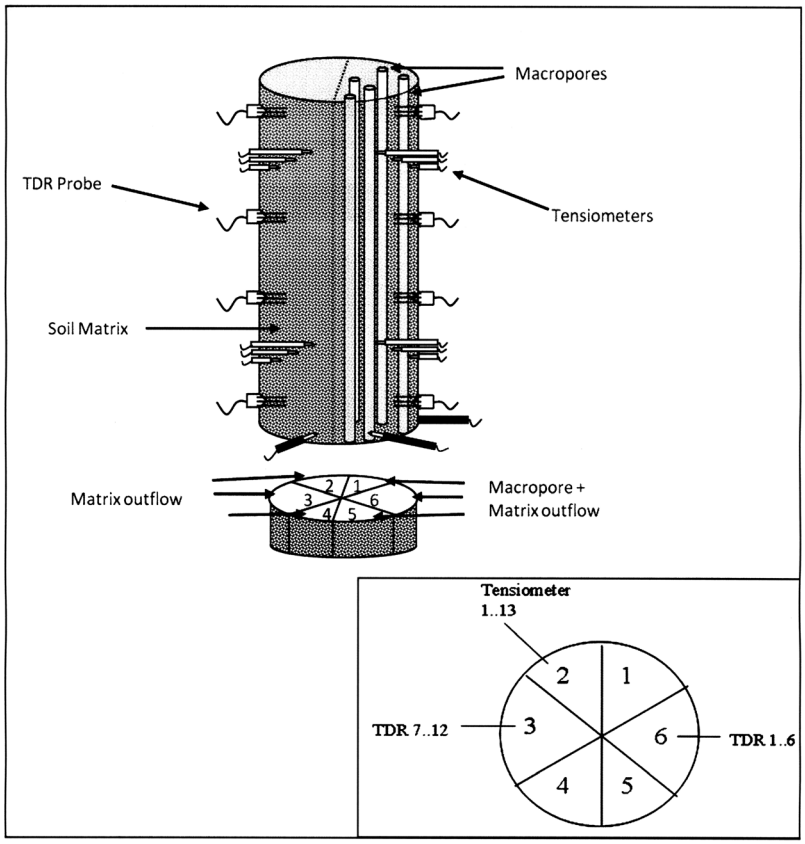

Figure 2. Schematic of the soil column with placement of TDRs and tensiometers in particular chambers.

20–25, 25–30, 30–35, 35–40, 40–45, 45–50, 50–55, 55–60, and 60–75 cm in the soil column. Drainage experiments were conducted by initially saturating the columns from the bottom. Upper and lower boundary conditions for infiltration and drainage experiments were set according to the transient flow conditions of the experiments (Table 1). Tracer transport studies using potassium bromide solution were conducted only on the high-density macropore column with 19 macropores, while initial bromide concentration in the column was considered to be zero.

4. Modeling Framework

4.1. Simulation Models

[16] Hydrus-1D [*Šimůnek et al.*, 2001, 2003] was used for all simulations. Single-porosity model (SPM), mobile-immobile model (MIM), and dual-permeability model with first-order (DPM1) and second-order (DPM2) water transfer functions were used to simulate flow and tracer transport experiments of the central and multiple-macropore columns. Among these, infiltration and drainage experiments were described by fitting the numerical solution of Richards' equation. The hydraulic conductivity function $K(h)$, which is required to solve the Richards equation, is described using a set of closed-form equations [*Mualem*, 1976; *van Genuchten*, 1980]:

$$K_d(h) = Ks_d \left(\frac{\theta(h) - \theta r_d}{\theta s_d - \theta r_d}\right)^{1} \left\{1 - \left[1 - \left(\frac{\theta(h) - \theta r_d}{\theta s_d - \theta r_d}\right)^{\frac{1}{m_d}}\right]^{m_d}\right\}^{2}, \tag{22}$$

$$\theta_d(h) = \theta r + \frac{\theta s_d - \theta r_d}{[1 + |\alpha_d h|^{n_d}]^{m_d}}, \tag{23}$$

$$m_d = 1 - \frac{1}{n_d}, \tag{24}$$

where d represents the matrix (m) or fracture (f) domains and $\theta(h)$ is the measured volumetric water content [$L^3\ L^{-3}$] at the suction h [L] that is taken positive for increasing suctions. The parameters θr and θs are the residual and saturated water contents [$L^3\ L^{-3}$], respectively; Ks is the saturated hydraulic conductivity [$L\ T^{-1}$]; and α [L^{-1}], n (dimensionless), m (dimensionless), and l (dimensionless) are empirical parameters determining the shape of the hydraulic conductivity functions. In particular, α [L^{-1}] is related to the inverse of the air entry suction, n (dimensionless) is a measure of the pore size distribution, and l (dimensionless) reflects pore discontinuity and tortuosity of the flow path.

[17] Tracer transport was described using CDE in the dominant pore regions as realized in Hydrus-1D for the specific conceptual model. For tracer transport simulations, bromide

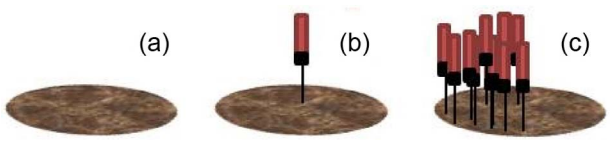

Figure 3. Experimental designs: (left) homogeneous soil, (middle) central macropore, and (right) multiple-macropore columns.

Table 1. Initial and Boundary Conditions as Specified at the Soil Surface ($z = L$) and Bottom of the Soil Profile ($z = 0$) for Different Experiments of the Soil Columns[a]

Columns	Experiment	Initial Condition[b]	Upper BC	Lower BC
Homogeneous soil column	infiltration	$h(L, 0) = -119$ cm, $h(d, 0) = h_0(d)$, $h(0, 0) = -42$ cm	$h(L, t) = 0$	$q(0, t) = 0$, if $h(0, t) < 0$ $h(0, t) = 0$, else[c]
	infiltration	$h(L, 0) = -155$ cm, $h(d, 0) = h_0(d)$, $h(0, 0) = -139$ cm	$h(L, t) = 6.5$ cm	$q(0, t) = 0$, if $h(0, t) < 0$ $h(0, t) = 0$, else[c]
	drainage	$h(L, 0) = 0.9$ cm, $h(d, 0) = h_0(d)$, $h(0, 0) = 68.6$ cm	$q(L, t) = 0$	$q(0, t) = 0$, if $h(0, t) < 0$ $h(0, t) = 0$, else[c]
Central macropore column	infiltration	$h(L, 0) = -186$ cm, $h(d, 0) = h_0(d)$, $h(0, 0) = -133$ cm	$h(L,0) < h(L, t_r) < h(L, T)$,[d] $h(L, t_r) = -186$ cm, .., 2 cm	$h(0,0) < h(0, t_r) < h(0, T)$. $h(0, t_r) = -133$ cm, …, −49 cm
Low-density macropore column	infiltration	$h(L, 0) = -209$ cm, $h(d, 0) = h_0(d)$, $h(0, 0) = -168$ cm	$h(L,0) < h(L, t_r) < h(L, T)$,[d] $h(L, t_r) = -209$ cm, .., 7 cm	$h(0,0) < h(0, t_r) < h(0, T)$. $h(0, t_r) = -168$ cm, …, −1 cm
High-density macropore column	infiltration	$h(L, 0) = -114$ cm, $h(d, 0) = h_0(d)$, $h(0, 0) = -45$ cm	$h(L,0) < h(L, t_r) < h(L, T)$,[d] $h(L, t_r) = -114$ cm, .., −17 cm	$h(0,0) < h(0, t_r) < h(0, T)$. $h(0, t_r) = -45$ cm, …, 23.5 cm
	drainage	$h(L, 0) = -9$ cm, $h(d, 0) = h_0(d)$, $h(0, 0) = 51$ cm	$h(L,0) < h(L, t_r) < h(L, T)$,[d] $h(L, t_r) = -9$ cm, .., −195 cm	$h(0,0) < h(0, t_r) < h(0, T)$. $h(0, t_r) = 51$ cm, …, −185 cm

[a]Symbols: h, pressure head; q, flux; z, vertical coordinate positive upward; L, column length; t, time; T, duration of the experiment.
[b]Equilibrium profile with h values linearly interpolated for depths between 0 and d, where d represents the tensiometer location.
[c]These conditions represent a seepage face boundary condition [*Šimůnek et al.*, 1998].
[d]Variable boundary condition with h values linearly interpolated for time between 0 and t_r, where t_r represents the time of tensiometer reading.

concentrations at all depths were normalized with respect to initially applied concentrations.

4.2. Model Parameterization

[18] To reduce the number of fitting parameters, some parameter values were fixed. Matrix and macropore tortuosity parameters were fixed at 0.5 [*Mualem*, 1976; *van Genuchten*, 1980; *Köhne et al.*, 2002]. Some of the matrix-macropore interface parameters (w_f, β, and a) for the central macropore and multiple-macropore columns were based on their geometry (e.g., for the high-density macropore column, a = 1.89 cm, $b = 0.05$ cm, $\zeta = 38.8$, $\beta = 0.67$, and $w_f = 3.3 \times 10^{-4}$ on the basis of equations (10), (16), and (17)). The γ_w value was fixed at 0.001 on the basis of soil mantle radii and estimated saturated hydraulic conductivity for the macropore domain [*Castiglione et al.*, 2003]. The bromide diffusion coefficient was calculated as 1.797 cm^2 d^{-1} [*Atkins*, 1990]. The rest of the model parameters were inversely estimated.

[19] Observations of matrix pressure head at three tensiometer locations and water content in both matrix and macropore domains at two TDR depths were the minimum data used for inverse analysis of water flow experiments. Bromide transport experiment of the 19 (high-density) macropore column utilized additional information on Br^- concentrations at a minimum of three depths for inverse modeling. A spatial discretization of 0.5 cm was adopted for all flow and transport modeling. An initial time step of 10^{-5} h and minimum and maximum time steps of 10^{-6} and 0.24 h were employed for both one- and two-domain model simulations.

[20] The inverse parameter estimation was performed by Levenberg-Marquardt minimization of the objective function φ [*Šimůnek et al.*, 1999]:

$$\varphi(\mathbf{b}) = \sum_{j=1}^{m} v_j \sum_{i=1}^{n} w_{i,j}\left[O_j(x, t_i) - E_j(x, t_i, \mathbf{b})\right]^2, \qquad (25)$$

where m is the total number of measurements; n is the number of observations in a particular measurement set; $O_j(x, t_i)$ is the observation at time i for the jth measurement set at location x; $E_j(x, t_i, \mathbf{b})$ are the corresponding estimated space-time variables for the vector $\mathbf{b}$ of optimized *van Genuchten* [1980] parameters; and v_j and $w_{i,j}$ are weighting factors associated with a particular measurement set or point, respectively. In this study, $w_{i,j}$ are set equal to 1 assuming similar error variances within a particular measurement set. Only data that are measured at larger time intervals and are underrepresented with respect to more frequent measurements require larger weights $w_{i,j}$. Then v_j is calculated for each simulation as [*Clausnitzer and Hopmans*, 1995]

$$v_j = \frac{1}{n_j \sigma_j^2}, \qquad (26)$$

which assumes that v_j is inversely related to the variance σ_j^2 within the jth measurement set and to the number of measurements n_j within the set.

4.3. Modeling Strategy

[21] Comparison of continuum-scale models and evaluation of inversely modeled parameters was done in the following manner. Inverse simulations were first performed with the homogeneous soil column to extract matrix-specific parameters. Then, keeping the matrix parameters fixed, macropore parameters were derived through inverse analysis of the experimental data of the central macropore column. To evaluate the suitability of these domain-specific parameters, forward simulations were performed with variably saturated flow and transport experiments of the low- and high-density multiple-macropore columns. Dual-permeability framework was used for inverse estimation of effective parameters from the central macropore column and for evaluation of multiple-macropore columns.

[22] For comparison among continuum-scale models (SPM, MIM, DPM1, and DPM2), inversely estimated soil hydraulic parameters were employed. Separate adjustments of parameters for each model were not done to prevent bias in comparison as fine-tuning of parameters would have enhanced agreement between predictions and observations.

4.4. Goodness-of-Fit Criteria

[23] Apart from graphical analysis, two statistical paramters were used for direct comparison between models and for evaluating best fit of parameters in inverse analysis.

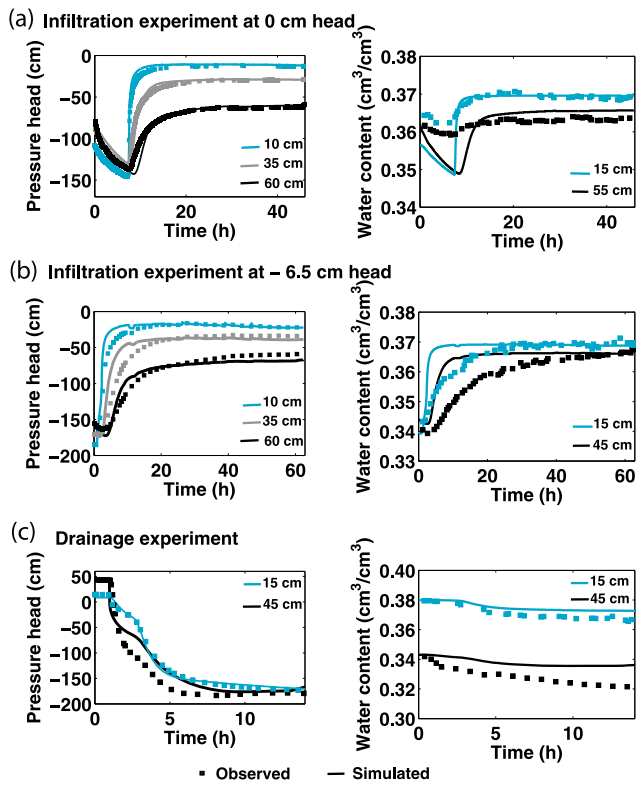

Figure 4. Simulated and observed pressure head and water content profiles for one drainage and two different infiltration experiments of the homogeneous soil column.

Modified coefficient of efficiency (E) and the mean absolute error (MAE) were used to obtain relative and absolute error estimates, respectively:

$$E = 1.0 - \frac{\sum_{i=1}^{N}\left[\left|O_j(x,t_i) - E_j(x,t_i,\mathbf{b})\right|\right]}{\sum_{i=1}^{N}\left[\left|O_j(x,t_i) - \overline{O}\right|\right]} \quad (27)$$

$$\mathrm{MAE} = 1.0 - \frac{\sum_{i=1}^{N}\left[\left|O_j(x,t_i) - E_j(x,t_i,\mathbf{b})\right|\right]}{N}, \quad (28)$$

where N is the total number of time steps and E is a normalized measure varying between minus infinity to 1.0. A value of $E = 1.0$ indicates perfect agreement between model and data, $E = 0$ indicates that the model is statistically as good as the observation mean in predicting the data, and $E < 0.0$ indicates an altogether questionable choice of model. E is a more conservative and reliable statistical measure and is less sensitive to extreme values as compared to commonly used goodness-of-fit measures such as the coefficient of determination (R^2) [*Legates and McCabe*, 1999]. In addition, an absolute error measure like the MAE carries the same units as the observations and is able to better assess the magnitude of deviation. A lower MAE and $E > 0.5$ typically signify better agreement between modeled and observed values.

5. Results and Discussion

5.1. Inverse Estimation of Matrix and Macropore Parameters

[24] Experimental observations and predictions of inverse modeling on flow experiments of the homogeneous soil column are documented briefly (Figure 4). One drainage and two infiltration experiments under transient flow conditions were used to infer soil hydraulic parameters of the matrix domain i.e., θr_m, θs_m, α_m, n_m, and Ks_m (Table 2). Figure 4 illustrates simulated and observed pressure head and water content profiles of the soil column for the respective durations of the experiments. The estimated soil hydraulic parameters for the matrix domain were able to reproduce sufficient details of the illustrated results. For example, the two humps in the pressure head curve (0–3.5 and 3.5–12 h) of the drainage experiment caused by pressure-controlled bottom boundary condition were sufficiently captured by the inversely estimated parameters. Moreover, the timing of rise (or fall) of soil matric potential was adequately captured by Hydrus-1D simulations for all three experiments. Simulated water content profiles showed considerable agreement with the measured values considering the fact that TDR measurements had a large variance and received lower weight in the objective function. Separate adjustments of parameters for simulating the wetting and drying cycles (i.e., hysteresis) in the infiltration and drainage experiments were not done in order to obtain a single set of effective matrix parameters. Moreover, parameter estimation from the three experiments qualified the judging criteria of $E > 0.5$ and low mean absolute error for both pressure head and water content measurements (Table 3).

[25] These estimated matrix parameters were then fixed to determine saturated hydraulic conductivity of the matrix-macropore interface (K_a) and macropore domain parameters (θr_f, θs_f, α_f, n_f, and Ks_f) from inverse simulations of the central macropore column experiments (Table 2). Figure 5 shows good conformity between simulated and measured

Table 2. Effective Soil Hydraulic Parameters and Corresponding 95% Confidence Limits for Low- and High-Density Macropore Columns Obtained From Inverse Modeling of Homogeneous and Single-Macropore Soil Columns

	Units	3-Macropore Low-Density Column	19-Macropore High-Density Column	95% Confidence Limits
Matrix Parameters (Obtained From Homogeneous Soil Column)				
θr_m	-	0.2	0.2	±0.029
θs_m	-	0.38	0.38	±0.005
α_m	cm^{-1}	0.004	0.004	±0.003
n_m	-	1.8	1.8	±0.326
Ks_m	cm h^{-1}	0.13	0.13	±1.998
l_m	-	0.5	0.5	-
Macropore Parameters (Obtained From Single-Macropore Column)				
θr_f	-	0.078	0.078	±0.066
θs_f	-	0.39	0.39	±0.001
α_f	cm^{-1}	0.01	0.01	±0.001
n_f	-	2	2	±0.354
Ks_f	cm h^{-1}	8.265	8.265	±0.001
l_f	-	0.5	0.5	-
Interface Parameters (Obtained From Geometry)				
w_f	-	5.2×10^{-5}	3.3×10^{-4}	-
β	-	0.54	0.67	-
γ_w	-	0.001	0.001	-
a	cm	4.85	1.89	-
Interface Parameter (Obtained From Single-Macropore Column)				
K_a	cm h^{-1}	4.174 (0.26[a])	4.174 (0.26[a])	±0.052

[a]Separately optimized value using higher weights for outflow measurements of the single-macropore column.

Table 3. Goodness-of-Fit Criteria for Inverse Estimation of Parameters From Homogeneous Soil and Single-Macropore Columns

Soil Column Type	Experiment	Modified Coefficient of Efficiency, E	Mean Absolute Error[a]
Homogeneous soil column	infiltration (0 cm head)	0.765	9.050 (0.011)
	infiltration (−6.5 cm head)	0.625	39.48 (0.227)
	drainage	0.761	12.205 (0.022)
Single-macropore column	infiltration	0.588	14.649 (0.038)

[a]MAE is reported with respect to pressure head (cm h^{-1}). MAE for water content measurements (cm^3 cm^{-3} h^{-1}) is given in parentheses.

pressure head, average water content, and matrix outflow profiles for a transient infiltration experiment of the central macropore column. It is worthwhile to mention that experimental observations correspond to pressure head values in the soil matrix domain, average water content values of matrix and macropore domains, and domain-specific outflow measurements. The conformity with macropore outflow is low as simulations suggest an immediate outflow while observations suggest the onset of outflow at 1.9 h, which is reasonable considering the height of the soil column (75 cm) and the fact that the soil was initially quite dry (Table 1). The dual-permeability model simulates flow from the macropore domain not only as a function of the flow capacity of the macropore but also as its exchange with the matrix domain. This interaction between the matrix and macropore domains is complex and is influenced by soil moisture retention characteristics of the unsaturated soil matrix, initial moisture conditions in both domains, geometry of macropores, and the conducting surface area of the interface region [*Weiler*, 2005]. The effect of this exchange is also visible as the predicted decrease in macropore flow at 8 h when predictions for matrix outflow begin (Figure 5). The rapid exchange predicted between the matrix and macropore domains and lack of outflow measurements in the objective function result in this nonconformity with macropore outflow. The inverse modeling exercise was repeated again with K_a as the only fitting parameter and inclusion of outflow measurements in the objective function. A decrease in K_a from 4.17 to 0.26 cm h^{-1} produced satisfactory results for all three observations (E = 0.588, MAE = 14.649 cm h^{-1} for pressure head, 0.0379 cm^3 cm^{-3} h^{-1} for water content, and 0.465 cm h^{-1} for outflow measurements). Note that water content in the macropore domain is predicted to be lower than in the matrix domain. This was observed for all soil depths and for other transient flow experiments as well (not shown here). The reasons for this will be discussed in section 5.2.

[26] The small differences observed between matrix and macropore domain results (pressure head and water content profiles) indicate that only mild physical nonequilibrium existed for the single-macropore column. The derived macropore domain and interface parameters were able to satisfactorily describe all flow experiments of the single (central) macropore column as per the goodness-of-fit criteria (Table 3).

5.2. Evaluation of Inversely Estimated Soil Hydraulic Parameters

[27] Multiple-macropore columns with 3 and 19 macropores were used to evaluate the accuracy of the derived domain-specific (matrix and macropore) and interface (K_a) parameters. As per Table 2, interface parameters based on macropore geometry (w_f, β, and a) were the only three variables different for the two multiple-macropore (low- and high-density) columns. The rest of the parameters were based on consistent values for matrix (θr_m, θs_m, α_m, n_m, and Ks_m), macropore (θr_f, θs_f, α_f, n_f, and Ks_f) and interface (K_a = 0.26 cm h^{-1}) regions obtained from inverse modeling of the homogeneous and single-macropore columns, as described in section 5.1. Forward modeling using modified Hydrus-1D was done for a transient infiltration experiment of the low-density macropore column. Matrix outflow and average water content measurements of the matrix and macropore domains for the simulated experiment agree well with the corresponding observations (Figure 6). Again, conformity with macropore outflow observations was found to be low and could be improved by separately fitting K_a (3.91 ± 1.001) and including outflow measurements in the objective function. Instead of separate adjustments to this parameter, the simultaneously fitted value of 4.17 cm h^{-1} from the single-macropore column was adopted to maintain consistency in our inverse estimation procedure (Table 3).

[28] For the high-density macropore column, infiltration, drainage, and bromide tracer experiments were conducted to test the performance of the estimated set of domain-specific (matrix and macropore) and interface (K_a = 4.17 cm h^{-1}) parameters (Figures 7 and 8). The agreement between pressure head profiles decreased with depth (all results not shown here) for both infiltration and drainage experiments. It is

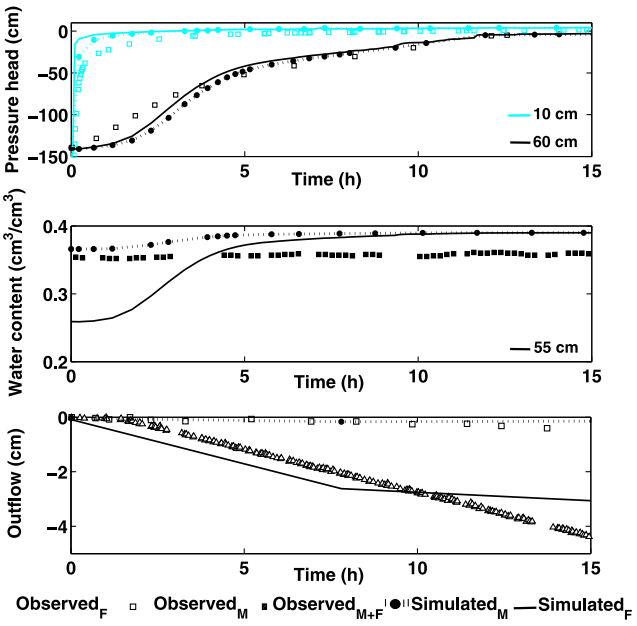

Figure 5. Simulated and observed pressure head, water content, and outflow profiles for a transient infiltration experiment of the central macropore column. Symbols: M, matrix domain; F, fracture or macropore domain; $M + F$, combined matrix and macropore domains.

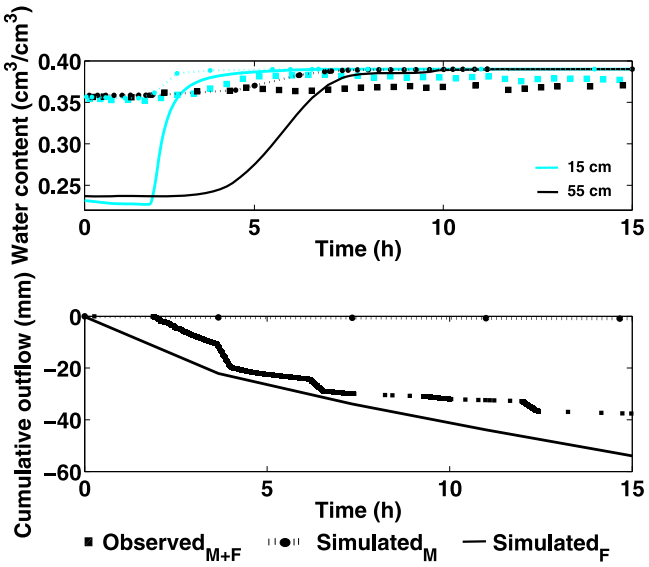

Figure 6. Simulated and observed (top) water content at 15 and 55 cm depths and (bottom) cumulative outflow of the low-density macropore column. Symbols: *M*, matrix domain; *F*, fracture or macropore domain; *M* + *F*, combined matrix and macropore domains.

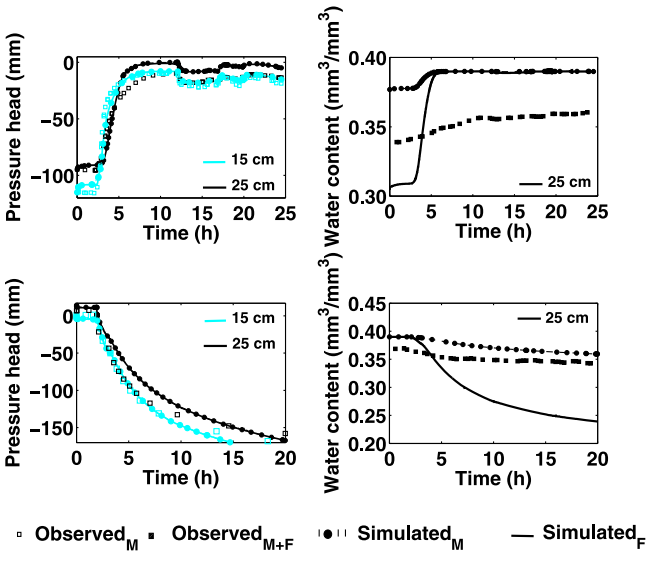

Figure 7. Simulated and measured pressure head and water content values for (top) infiltration and (bottom) drainage of the high-density macropore column. Symbols: *M*, matrix domain; *F*, fracture or macropore domain; *M* + *F*, combined matrix and macropore domains.

possible that in the multiple-macropore column the lateral water transfer rate needs to be adjusted to better explain the mismatch between higher predictions and lower observations of pressure head in the lower depths of the soil column. Incorrect quantification of lateral water transfer is also the reason for lower water content predictions in the macropore domain as compared to the soil matrix. Observations of lower water transfers (e.g., due to clogging of pores or soil aggregate coatings) between the fracture and matrix domains have been reported in various experimental settings [*Gerke and Köhne*, 2004; *Kodešová et al.*, 2008]. This could be a result of clogging of pores as observed in certain experiments of the single-macropore column [*Castiglione et al.*, 2003] or simply for maintaining the continuity of pressure potential across the large number of laterally distributed macropores of the multiple-macropore columns. Nevertheless, the domain-specific parameters were able to effectively capture the trend in pressure head profiles at all depths during forward simulations of the two transient flow experiments (Figure 7). Unlike pressure head profiles, the rise in bromide concentrations was not suitably captured even at shallow depths (Figure 8). The matching criteria attributed good performance to inversely estimated parameters for flow in both the low- and high-density multiple-macropore columns but not to bromide transport ($E = -16.777$) in the high-density macropore column (Table 4). Separate adjustments to K_a produced an unsatisfactory match to tracer concentration data. It is noteworthy, however, that the bromide transport experiment was well explained with changes in only the saturated hydraulic conductivity of the matrix domain (Ks_m) (i.e., from 0.13 to 0.40 cm h^{-1}). The increment in *Ks* is well explained by *Freeze* [1975], who reports that saturated hydraulic conductivity is likely a function of the boundary conditions and soil structure and macropore geometry in the case of statistically heterogeneous soils. In our study, structural heterogeneity arises from the use of domain-specific parameters of the homogeneous and single-macropore columns on multiple-macropore columns with different densities and distributions of macropore. It should be stated up front that we do not consider the changes in Ks_m as calibration of the model on the basis of observed data but rather as an evaluation of desired variability in parameters in order to account for increase in macropore density. Since saturated hydraulic conductivity produces the most sensitivity to preferential flow results and has an important bearing on contaminant transport [*Zhang et al.*, 2006], it is feasible that only this parameter required evaluation through inverse modeling.

5.3. Parameter Identification and Uniqueness

[29] Problems of nonuniqueness, identifiability, and ill posedness are often encountered when dealing with simultaneous estimation of soil hydraulic parameters using inverse

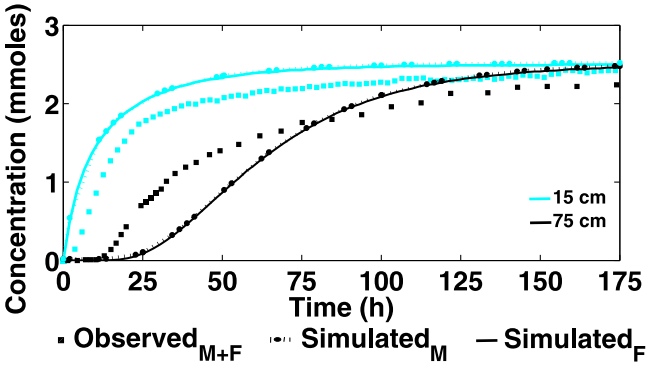

Figure 8. Simulated and measured bromide concentration values for a solute transport experiment of the high-density macropore column. Symbols: *M*, matrix domain; *F*, fracture or macropore domain; *M* + *F*, combined matrix and macropore domains.

Table 4. Goodness-of-Fit Criteria for Estimated Parameters of the Multiple-Macropore Columns

Soil Column Type	Experiment	Modified Coefficient of Efficiency, E	Mean Absolute Error[a]
Low-density macropore column	infiltration	0.686	24.327 (12.029)
High-density macropore column	infiltration	0.899	7.236 (0.039)
	drainage	0.806	7.019 (0.044)
	bromide transport (before inverse solution)	−16.777	8.968[b]
	bromide transport (after inverse solution)	0.662	0.164[b]

[a]MAE is reported with respect to pressure head (cm h^{-1}). MAE for water content measurements (cm^3 cm^{-3} h^{-1}) is given in parentheses.
[b]MAE corresponds to bromide concentration (mmol h^{-1}).

modeling. To test the uniqueness of the inverse method, (1) examination of parameter correlations was conducted, (2) confidence intervals were evaluated for each parameter, and (3) parameter estimation was done using combinations of different starting values for all soil hydraulic parameters.

[30] For the homogeneous soil column, one transient infiltration experiment revealed high correlation ($|r| > 0.75$) between α_m and n_m and the other revealed no correlation, while the drainage experiment revealed high correlation between α_m and θs_m parameters (Table 5). Since α_m was the common parameter and had a low confidence interval (Table 2), all three simulations were repeated with this parameter initialized at ±30% of its originally optimized value. Several combinations of α_m (±30%) with θs_m and n_m fixed at originally optimized values and at different starting values were carried out. The final optimized parameters were either the same or within the confidence intervals of their original values (Table 2). As an example, with lower α_m (−30%) values, the final optimized parameters (the original values are given in parentheses) are given as θr_m = 0.2 (0.2), θs_m = 0.4 (0.38), α_m = 0.003 (0.004), n_m = 1.8 (1.8), and Ks_m = 0.10 (0.13). Table 5 further suggests a high correlation between α_f and n_f parameters using inverse modeling of the single-macropore column, indicating that their simultaneous estimation did not yield unique results. Independent estimation of these parameters would yield lower uncertainty and better results. We fixed α_f at 0.33 on the basis of capillary bundle theory for a single macropore of 1 mm which did not produce satisfactory match of the data (E = −1.007, MAE = 104.968 cm h^{-1} for pressure head and MAE = 0.348 cm^3 cm^{-3} h^{-1} for water content measurements). Mild nonequilibrium conditions observed in the single-macropore column could have resulted in the existence of highly correlated macropore domain parameters (α_f and n_f) [*Zurmühl and Durner*, 1998]. Since all experiments produced mild nonequilibrium differences for this column, α_f and n_f were treated as fitting parameters of the van Genuchten-Mualem model and varied at ±30% of their original values. Again, the final optimized parameter values were within ±10% of their original values.

[31] Table 2 suggests small confidence intervals for all soil hydraulic parameters of the matrix domain except Ks_m. One reason for high uncertainty in saturated hydraulic conductivity parameter (Ks_m) stems from establishing a best compromise parameter set to satisfy observations of different types of experiments. The effects of hysteresis were ignored to arrive at this best set of optimized soil hydraulic parameters since both infiltration and drainage experiments were used for inverse estimation. In this regard, confidence intervals for the macropore (θr_f, θs_f, α_f, n_f, and Ks_f) and interface region (K_a) parameters were generally small and were derived from a

Table 5. Correlation Between Inversely Estimated Soil Hydraulic Parameters[a]

Soil Column	Experiment		Soil Hydraulic Parameters					
			θr	θs	α	n	Ks	K_a
Homogeneous soil column	infiltration (0 cm head)[b]	θr_m	1					
		θs_m	0.0	1				
		α_m	0.0	0.0	1			
		n_m	0.0	0.0	0.0	1		
		Ks_m	0.0	0.0	0.0	0.0	1	
	infiltration (6.5 cm head)	θr_m	1					
		θs_m	−0.060	1				
		α_m	0.324	−0.031	1			
		n_m	−0.568	−0.022	**0.948**	1		
		Ks_m	−0.722	0.057	0.668	0.716	1	
	drainage	θr_m	1					
		θs_m	−0.383	1				
		α_m	0.382	**−0.995**	1			
		n_m	−0.016	−0.101	0.101	1		
		Ks_m	−0.489	0.386	−0.384	0.002	1	
Single-macropore column[c]	infiltration	θr_f	1					
		θs_f	−0.275	1				
		α_f	0.498	−0.293	1			
		n_f	0.406	−0.362	**0.925**	1		
		Ks_f	−0.235	0.267	−0.272	−0.571	1	
		K_a	0.345	−0.042	−0.255	−0.028	−0.295	1

[a]Bold indicates high correlation with $|r| > 0.75$.
[b]The correlations for this experiment were of the order of 10^{-15}.
[c]The soil hydraulic parameters for this column represent the macropore domain.

Table 6. Soil Hydraulic Parameters of the Single- and Multiple-Macropore Columns Used for Different Conceptual Models (SPM, MIM, and DPM)

		Soil Hydraulic Parameters																
		Matrix or Immobile Region						Macropore or Mobile Region						Interdomain Transfer				
Soil Column	Model	θr	Θs	α	n	Ks	l	θr	θs	α	n	Ks	l	w_f	β	γ_w	a	K_a
Single-macropore column	SPM	0.2	0.38	0.004	1.8	0.13	0.5											
	MIM	0.2	0.38					0.08	0.39	0.01	2	8.27	0.5	1.7×10^{-5}				
	DPM	0.2	0.38	0.004	1.8	0.13	0.5	0.08	0.39	0.01	2	8.27	0.5	1.7×10^{-5}	0.45	0.001	11.95	0.26
Low-density macropore column	SPM	0.2	0.38	0.004	1.8	0.13	0.5											
	MIM	0.2	0.38					0.08	0.39	0.01	2	8.27	0.5	5.2×10^{-5}				
	DPM	0.2	0.38	0.004	1.8	0.13	0.5	0.08	0.39	0.01	2	8.27	0.5	5.2×10^{-5}	0.54	0.001	4.85	4.17
High-density macropore column	SPM	0.2	0.38	0.004	1.8	0.13*	0.5											
	MIM	0.2	0.38					0.08	0.39	0.01	2	8.27	0.5	3.3×10^{-4}				
	DPM	0.2	0.38	0.004	1.8	0.13*	0.5	0.08	0.39	0.01	2	8.27	0.5	3.3×10^{-4}	0.67	0.001	1.89	4.17

single infiltration experiment. Note that n_f has moderate uncertainty due to its correlation with α_f.

[32] As suggested earlier, all inverse modeling simulations were repeated with different initial parameter values, resulting in final values within ±10% of the original optimized values. As an example, with higher n_m (+30%) values, the final optimized parameters (the original values are given in parentheses) are given as θr_m = 0.212 (0.2), θs_m = 0.365 (0.38), α_m = 0.0044 (0.004), n_m = 1.88 (1.8), and Ks_m = 0.136 (0.13), while lower θs_f gave the following results: θr_f = 0.053 (0.08), θs_f = 0.36 (0.39), α_f = 0.009 (0.01), n_f = 1.8 (2), Ks_f = 8 (8.27), and K_a = 0.27 (0.26).

[33] Overall, the inverse modeling approach produces acceptable representation of the data and is suitable for estimation of most of the soil hydraulic parameters. We do believe that independent estimation of soil hydraulic parameters and adding data of the same or different types of measurement can improve inverse estimation. Note that we defined the objective function using two different sets of measurements: pressure head response and water content profiles (also bromide concentration, wherever appropriate) at different depths of the experimental soil columns. We found that addition of outflow measurements improved inverse estimation in both homogeneous soil and single-macropore columns. Our analysis indicates that inverse optimization runs with simultaneous optimization of parameters consistently converged to similar parameter values, indicating uniqueness of the inverse problem. However, uncertainty in soil hydraulic parameters needs to be further evaluated to better account for preferential flow processes and lateral exchange between the two domains. This is the subject of a parallel study which compares the conventional and adaptive Metropolis-Hastings algorithm in simulating correlated soil hydraulic parameters of the matrix and macropore domains and evaluates the output uncertainty associated with them.

5.4. Comparison of Models

[34] The inversely estimated parameters derived using dual-permeability formulation were subsequently used for comparison between the single-porosity model (SPM), mobile-immobile model (MIM), and dual-permeability model (DPM) for simulating preferential flow and transport through the single- and multiple-macropore columns (Table 6). Note that single and higher density macropore columns differ only in the parameterization of the interface region including the fitted K_a. DPM1 and DPM2 were evaluated with similar parameters because they differ in their treatment of water transfer functions only (equations (12) and (15)). Accuracy of model predictions could have been enhanced with separate parameter adjustments for each model, but the aim of this analysis is to evaluate best model performances under conditions of different macropore distributions. Therefore, consistency in parameter values was maintained across different conceptual models.

5.5. Single-Macropore Column

[35] Results for experiments other than those used for inverse analysis are shown below. Figure 9 illustrates simulations of continuum-scale models (SPM, MIM, and DPM1) and observations of pressure head and water content profiles at 25 cm depth of the single-macropore column for a transient infiltration experiment. MIM is found to overestimate both pressure head and water content profiles at the given depth as it incorporates flow through the higher-flowing domain, i.e., macropore (mobile) region. Single-porosity model and matrix domain of the dual-permeability model (DPM_M) give comparable results because SPM works with the matrix domain as the sole flow medium in this study. DPM_M and the fracture or macropore domain of the dual-permeability model (DPM_F) showed minute variations in their results given the mild nonequilibrium conditions observed in the central macropore column.

[36] Both SPM and DPM satisfied the goodness-of-fit criteria in simulating preferential flow experiments of the single-macropore column (Table 7). The choice of MIM to simulate the infiltration experiment is questionable with our criteria of $E < 0.5$. It seems that MIM overestimates flow from soil matrix (immobile) to the macropore (mobile) as it quantifies exchange between the two regions on the basis of relative saturation differences (equation (5)). According to the capillary bundle theory, flow from matrix to a macropore of size 1 mm is justified when water entry pressure is close to −1.48 cm, which implies that the surrounding soil matrix should be close to saturation. Our initial conditions indicate that the soil matrix is quite dry (Table 1) when MIM predicts this exchange, and this is an inherent limitation of the exchange term used in this model. On the other hand, MIM statistically outperforms SPM and DPM in simulating the drainage experiment, which is reasonable as drainage occurs through the largest pore first. However, graphical interpretation suggests that average outflow measurements

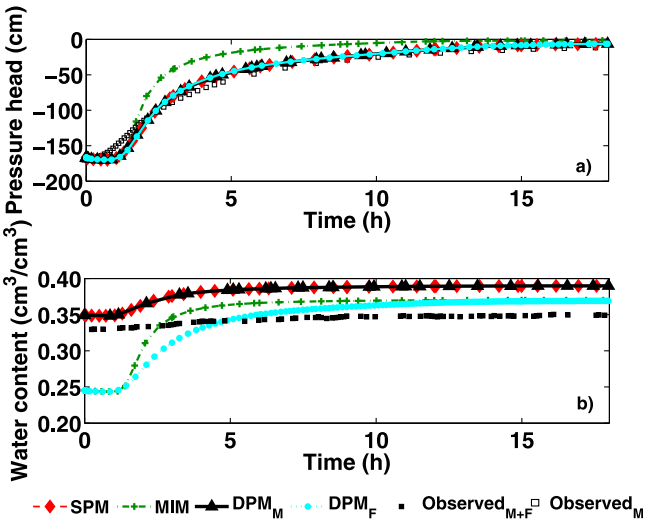

Figure 9. Observed and simulated results for infiltration experiment of the central macropore column: (a) pressure head and (b) water content at 25 cm depth. Symbols: *M*, matrix domain; *F*, fracture or macropore domain; *M* + *F*, combined matrix and macropore domains.

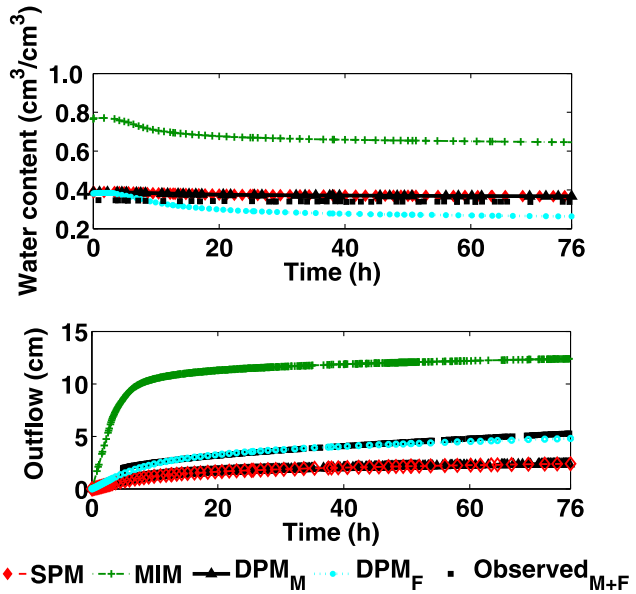

Figure 10. Observed and simulated results for drainage experiment of the central macropore column: (top) water content at 55 cm depth and (bottom) outflow at 75 cm. Symbols: *M*, matrix domain; *F*, fracture or macropore domain; *M* + *F*, combined matrix and macropore domains.

for the drainage experiment were described appropriately by DPM only (Figure 10). MIM overestimated and SPM underestimated outflow from the bottom of the soil column. DPM also gave a better match to observations of average water content profiles of the two domains for both experiments (Figures 9 and 10).

5.6. Multiple-Macropore Columns

[37] Figure 11 depicts pressure head results for a transient infiltration experiment of the high-density multiple-macropore column. The pressure head profiles at 10, 20, and 30 cm showcase equivalent results for all models. However, the trend of the pressure head profile is best captured by DPM at all depths (see Figure 11, inset). Similarly, observations of average water content at all depths and outflow for a transient drainage experiment are well described by DPM, whereas MIM overpredicts and SPM underpredicts both types of observations (Figure 12). It is apparent that SPM and MIM act according to their parameterization of the low (matrix) and high (macropore) flowing domains, respectively.

[38] The bromide transport experiment also validates the appropriateness of DPM in simulating preferential transport in the multiple-macropore columns. Figure 13 shows concentration profiles at 25 and 35 cm simulated using different models with the adjusted Ks_m parameter (0.4 cm h^{-1}) instead of the effective value (0.13 cm h^{-1}). Since the adjusted Ks_m value is kept constant for all conceptual models, it does not affect our comparison of model performances. In Figure 13, SPM produced results close to DPM_M, yet the rising limb of the solute concentration graph was captured by DPM only (see Figure 13, inset). This is important from a contaminant transport perspective as knowledge about initial breakthrough is crucial in assessing groundwater vulnerability to potential contamination. SPM and MIM failed to satisfy the goodness-of-fit criteria for this experiment with $E < 0.0$ (Table 7).

[39] Similar to results of the high-density (19) macropore column, DPM gave better results for the experiments of the low-density (3) macropore column and surpassed SPM and MIM in model performance criteria (Table 7). Unlike results for the single-macropore column, DPM consistently performed better for all types of experiments of the multiple-macropore columns (Table 7). Statistically, the model performance was unacceptable for MIM for the transient infiltration experiment of the low-density macropore column.

Table 7. Goodness-of-Fit Criteria for Comparison of Models

		SPM		MIM		DPM	
Soil Column Type	Experiment	*E*	MAE[a]	*E*	MAE[a]	*E*	MAE[a]
Single macropore	infiltration	0.517	9.104 (0.036)	0.102	16.628 (0.335)	0.598	9.387 (0.028)
	drainage	0.852	5.450 (0.017)	0.939	1.927 (0.320)	0.852	5.465 (0.017)
Low-density macropore	infiltration	0.637	24.741 (14.666)	−0.071	50.861 (0.399)	0.686	24.327 (12.029)
High-density macropore	infiltration	0.804	7.337 (0.031)	0.739	6.107 (0.373)	0.899	7.236 (0.039)
	drainage	0.802	7.103 (0.070)	0.730	5.939 (0.306)	0.806	7.019 (0.044)
	bromide transport[b]	−1.294	1.279	−2.881	1.963	0.662	0.164

[a]MAE is reported with respect to pressure head (cm h^{-1}). MAE for water content measurements (cm^3 cm^{-3} h^{-1}) is given in parentheses.
[b]MAE corresponds to bromide concentration (mmol h^{-1}).

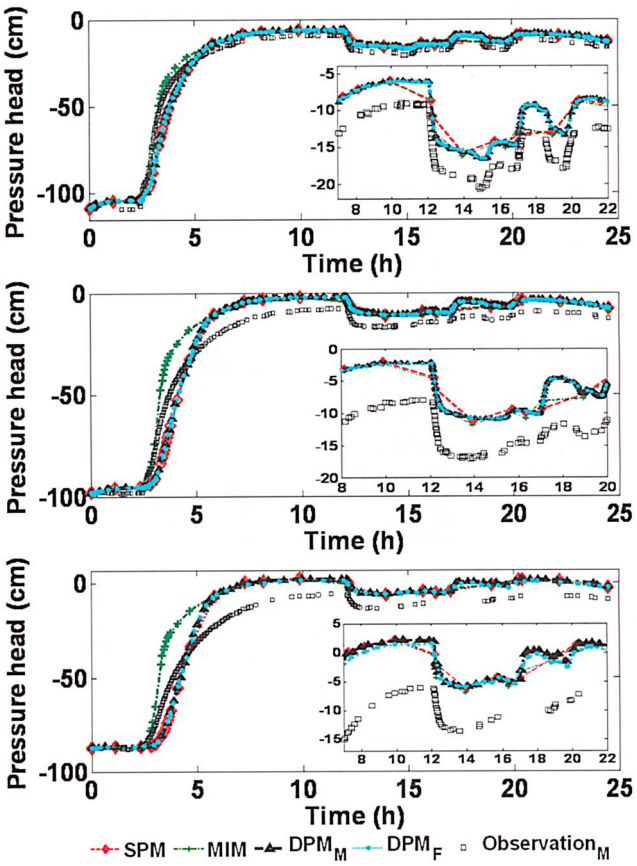

Figure 11. Simulated and observed pressure head profiles at (top) 10, (middle) 20, and (bottom) 30 cm for an infiltration experiment of the high-density multiple-macropore column. Symbols: *M*, matrix domain; *F*, fracture or macropore domain.

5.7. DPM1 Versus DPM2

[40] Comparison of DPM1 and DPM2 showed only slight variation in simulating infiltration and drainage experiments of the single- and multiple-macropore columns (Figures 14 and 15). The performance criteria substantiated DPM1 to perform slightly better than DPM2 in experiments of the multiple-macropore columns (not shown here). It is possible that the choice of a single-domain representation for 19 (3) macropores causes the models to neglect lateral transfers between individual macropores and focus more on the vertical flow through them. This error in analysis (ε_a) is more for DPM2 because of the second-order characteristic of the water transfer function:

$$\varepsilon_a = \Gamma_{\text{act}} - \Gamma_{\text{sim}}, \tag{29}$$

where Γ_{act} and Γ_{sim} are the actual and simulated transfer rates [T^{-1}], respectively. The corresponding errors for DPM1 and DPM2 can be obtained from equations (12), (13), and (15) as

$$\varepsilon_a^{\text{DPM1}} = \Gamma_{\text{act}} - \Gamma_{\text{sim}}^{\text{DPM1}} = \Gamma_{\text{act}} - \frac{\beta K_a \gamma_w}{a^2}\left(h_f - h_m\right) \tag{30}$$

$$\varepsilon_a^{\text{DPM2}} = \Gamma_{\text{act}} - \Gamma_{\text{sim}}^{\text{DPM2}} = \Gamma_{\text{act}} - \frac{\beta K_a}{2a^2}\frac{\left(h_f - h_m\right)\left[\left|h_m - h_i\right| - \left|h_f - h_i\right|\right]}{\left|h_m - h_i\right|}. \tag{31}$$

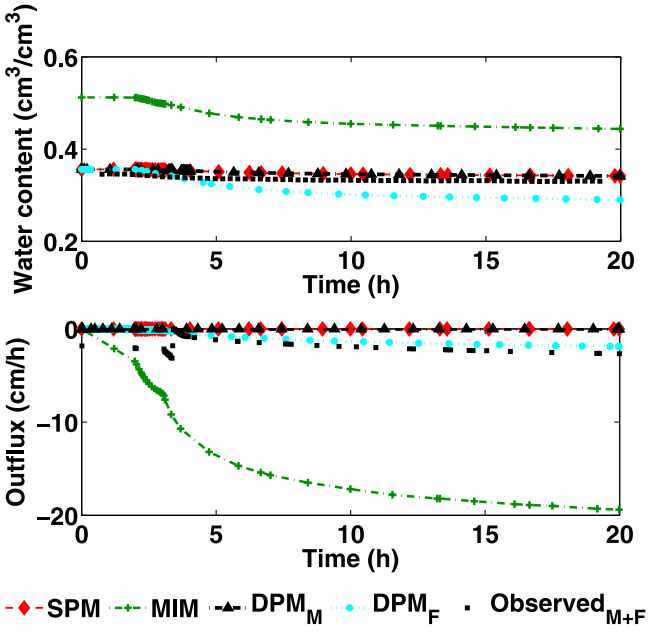

Figure 12. Simulated and observed (top) water content at 5 cm and (bottom) outflow for a drainage experiment of the high-density multiple-macropore column. Symbols: *M*, matrix domain; *F*, fracture or macropore domain; *M* + *F*, combined matrix and macropore domains.

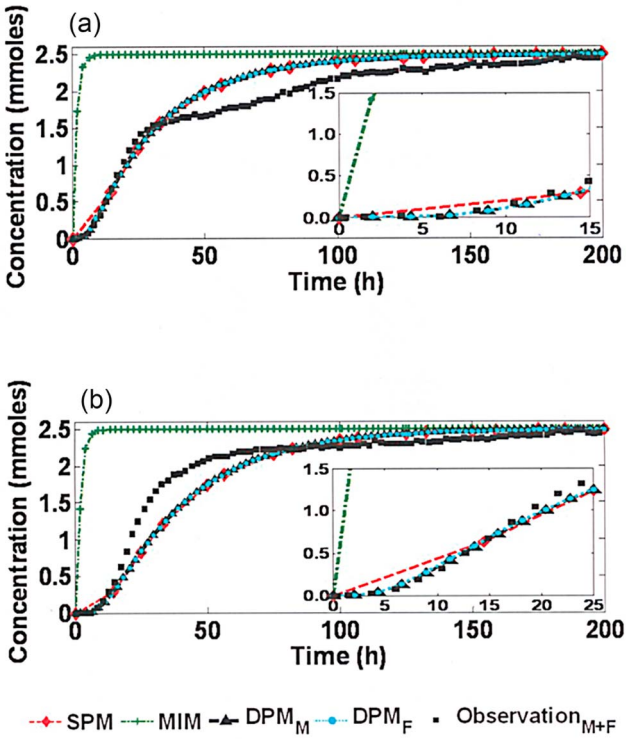

Figure 13. Simulated and observed bromide concentration profiles at (a) 25 and (b) 35 cm for a tracer transport experiment of the multiple-macropore column with 19 macropores. Symbols: *M*, matrix domain; *F*, fracture or macropore domain; *M* + *F*, combined matrix and macropore domains.

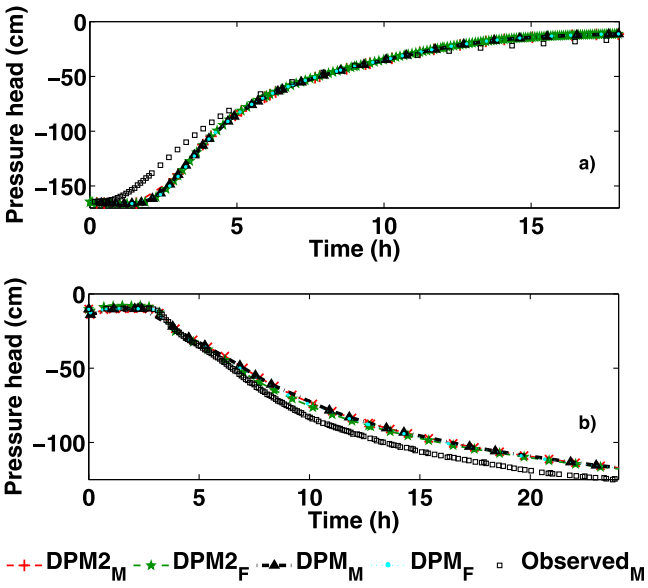

Figure 14. Simulated and observed pressure head profiles at 35 cm depth for (a) infiltration and (b) drainage experiments of the central macropore column. Symbols: *M*, matrix domain; *F*, fracture or macropore domain.

Considering the entirely similar effective parameter set for DPM1 and DPM2 and the use of lumped observations of the macropore domain, the order of the error is reduced to

$$\varepsilon_a^{\mathrm{DPM1}} = \varepsilon(h_f - h_m) \cong O(1) \tag{32}$$

$$\varepsilon_a^{\mathrm{DPM2}} = \varepsilon\left((h_f - h_m)\frac{[|h_m - h_i| - |h_f - h_i|]}{|h_m - h_i|}\right) \cong O(2). \tag{33}$$

The difference in performance of DPM2 is trivial when lumped data sets are used as the disparity between DPM1 and DPM2 was small to begin with (Figure 15). However, this substantiates the significance of using domain-specific measurements to reduce errors while using numerically efficient models and to improve predictions of preferential flow and transport.

5.8. Best Model Performance

[41] Proper evaluation of continuum-scale models in predicting contaminant transport under different macropore densities is important for quantifying agricultural pollution via preferential flow paths. The use of consistent matrix and macropore values instead of fitted parameters across the different conceptual models heightens the problem of choosing a superior model. For the case of a single (central) macropore column, the choice of a better model between DPM and SPM for simulating infiltration and between DPM and MIM for simulating drainage remains open primarily because of the mild nonequilibrium conditions observed in this column. Judging from statistical criteria, DPM has a consistently better fit in both the low- and high-density multiple-macropore columns than in case of the single-macropore column (Table 7). This is especially true for the bromide transport experiment in which SPM and MIM failed to satisfy the goodness-of-fit criteria. The predictive performance of DPM is reflected in its superiority in simulating average water content profiles at different depths, simulating outflow from the bottom, and reproducing temporal patterns of pressure head and bromide breakthrough from the high-density multiple-macropore column. This suggests that the density of the macropore is important in determining the complexity of the model employed. As we move from the central macropore column with a single macropore (1 mm diameter) to the multiple-macropore columns with 3 (low-density) and 19 (high-density) macropores of similar size, a continuum-scale model with higher complexity is essential in accurately predicting preferential water and bromide transport.

6. Limitations of the Study

[42] Despite the comprehensive data set and advanced conceptual models used in this study, there are certain limitations to our approach. First, this study does not evaluate the effect of using objective functions with different formulations and weightings on parameterizing the conceptual models or in quantifying preferential flow from the experimental data. Several studies have shown that the choice of objective functions can alter parameter estimates, parameter uncertainty bounds, and predictive capabilities of the model [*Vrugt et al.*, 2003; *Schoups and Vrugt*, 2010]. Our results containing objective functions with and without outflow measurements also suggest that different combinations of objective functions could lead to improvement in hydrologic predictions. We believe that evaluating likelihood functions and assessing their effect on parameter and prediction uncertainty is beyond the scope of the current study and encourage users to evaluate their objective functions before transferring results from our study.

[43] Second, the two-domain conceptual models used in this study are assumed to represent hydraulic properties of the matrix (immobile) and macropore (mobile) domains. Experimental methods to determine hydraulic functions or water retention characteristics of individual domains within multidomain configuration are nonexistent [*Köhne et al.*, 2009]. Therefore, these hydraulic properties are determined by collecting data from transient experiments and inversely estimating parameters of the individual domains. This traditional approach assumes a spatially homogeneous region (domain) with uniform hydraulic properties, while the observations represent a point measurement in space or time. If the

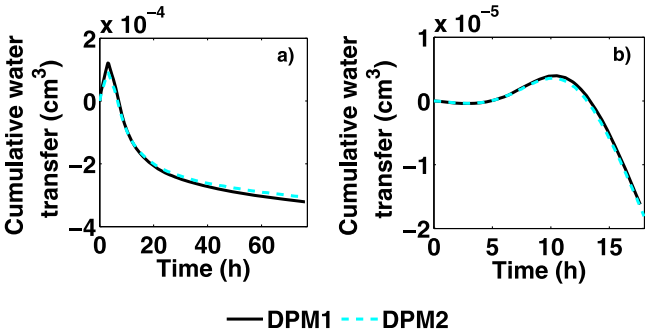

Figure 15. Cumulative water transfer for (a) infiltration and (b) drainage experiments of the high-density multiple-macropore column.

observations do not satisfy the ergodicity assumption, the validity of using this traditional approach for estimating domain-specific parameters becomes questionable [*Wu et al.*, 2005; *Yeh et al.*, 2005]. For this scenario, *Yeh et al.* [2005] developed a spatial moment analysis that can be employed to derive effective parameters using observations of spatial and temporal variations in water content within the individual domains. Since this study lacks data on spatiotemporal variations within each domain under transient flow conditions, it is impossible to investigate the effect this spatial distribution (of macropores) has on effective parameters for individual domains. Moisture diffusivity length and the scale of the dominant heterogeneity, which in this case is the lateral distribution of macropores, will affect the disparity between model predictions and experimental observations. However, improved experimental techniques and an intensive data set are still required to prove or disprove the effect areal variations in macropore density have on effective domain-specific parameters.

7. Conclusions

[44] This study evaluates whether transport behavior of macropores is a function of its density and examines the variability required (if any) in soil hydraulic parameters to account for changes in macropore density. This has serious implications for agricultural soils, where crop and management activities such as mechanized farming, irrigation scheduling, crop rooting characteristics, and earthworm activity change macropore density at various times during a season and affect leaching of agrochemicals via preferential flow paths. For this study, domain-specific soil hydraulic parameters were inversely estimated from designed soil columns of representative flow domains (homogeneous and central macropore) and were used for predicting preferential flow under different macropore distributions (single macropore and low- and high-density macropore columns) and transient flow conditions. Results indicate that inversely estimated parameters are successful in describing preferential flow but not tracer transport in both types (low and high density) of multiple-macropore columns. Preferential bromide transport for the high-density macropore column could be predicted with adjustments in saturated hydraulic conductivity of the matrix domain (Ks_m) only. Saturated hydraulic conductivity is likely a function of the boundary conditions and soil geometry in the case of statistically heterogeneous soils [*Freeze*, 1975]. In this study, structural heterogeneity stems from the use of consistent domain-specific parameters of the homogeneous and central macropore columns on low- and high-density multiple-macropore columns. The variation in one soil hydraulic parameter (Ks_m) is expected on account of increase in macropore density from single-macropore column to multiple-macropore columns. Other studies have indicated lower saturated hydraulic conductivities and mismatch with predictions due to the presence of a large number of closely spaced macropores [*Ahuja et al.*, 1995; *Kramers et al.*, 2005]. We believe that this refinement in inversely estimated Ks_m is required to account for lateral exchange between matrix and macropore domains as a result of high density of macropores and to accurately quantify preferential transport in such soils. Also, proper description of this lateral exchange process using soil hydraulic parameters was found to be crucial in correctly representing outflow from the macropore domain for all macropore columns. Future studies are needed to evaluate the specific contribution and sensitivity of the different soil hydraulic parameters to this interaction.

[45] A performance evaluation of continuum-scale models including the single-porosity model (SPM), mobile-immobile model (MIM), and dual-permeability model (DPM) with first- and second-order between-domain water transfer functions that employed these inversely estimated matrix and macropore parameters is also conducted. Judging from statistical criteria, the dual-permeability model was able to successfully reproduce the preferential flow characteristics of the single- and multiple-macropore columns in a deterministic framework. Further evaluation suggests that it was able to predict the initial rise (or fall) of pressure head and bromide concentration for the different experiments of the columns, which bears significance in early predictions of contaminant transport and prevention of potential contamination. Intercomparison of models indicates that increasing model complexity from SPM to MIM to DPM improves the description of preferential flow phenomenon in the multiple-macropore columns but not in the central macropore column. This suggests that the use of a more complex model is recommended with increase in macropore density to accurately capture all the dynamics of the system, including depth profiles, temporal trends, and breakthrough curves.

[46] Including lumped observations of pressure head, water content, cumulative outflow, and effluent concentration for the matrix and macropore domains into the objective function of DPM2 enhanced errors in model parameters because of the second-order characteristic of the water transfer function. This suggests that domain-specific measurements should be used wherever available to reduce errors when using numerically efficient models. Both macropore density and availability of domain-specific data seem to have an important bearing on the complexity of the model employed.

[47] **Acknowledgments.** This project was supported by the National Science Foundation (grant EAR 0635961). We thank P. Castiglione and J. M. Köhne for valuable comments and suggestions during the study. This research was partly supported by award 5R01ES015634 from the National Institute of Environmental Health Sciences. The content is solely the responsibility of the authors and does not necessarily represent the official views of the National Institute of Environmental Health Sciences or the National Institutes of Health.

References

Abbasi, F., J. Šimůnek, J. Feyen, M. T. van Genuchten, and P. J. Shouse (2003), Simultaneous inverse estimation of soil hydraulic and solute transport parameters from transient field experiments: Homogeneous soil, *Trans. ASAE*, *46*(4), 1085–1095.

Ahuja, L. R., and C. Hebson (1992), Root zone water quality model, *GPSR Tech. Rep. 2*, Agric. Resour. Serv., U.S. Dep. of Agric., Fort Collins, Colo.

Ahuja, L. R., K. E. Johnsen, and G. C. Heathman (1995), Macropore transport of a surface-applied bromide tracer: Model evaluation and refinement, *Soil Sci. Soc. Am. J.*, *59*, 1234–1241, doi:10.2136/sssaj1995.03615995005900050004x.

Atkins, P. W. (1990), *Physical Chemistry*, 4th ed., 995 pp., W. H. Freeman, New York.

Beven, K., and P. Germann (1982), Macropores and water flow in soils, *Water Resour. Res.*, *18*, 1311–1325, doi:10.1029/WR018i005p01311.

Biggar, J. W., and D. R. Nielsen (1962), Miscible displacement: II. Behavior of tracers, *Soil Sci. Soc. Am. J.*, *25*, 1–25.

Böhlke, J.-K. (2002), Groundwater recharge and agricultural contamination, *Hydrogeol. J.*, *10*, 153–179, doi:10.1007/s10040-001-0183-3.

Brusseau, M. L., and P. S. C. Rao (1990), Modeling solute transport in structured soils: A review, *Geoderma*, *46*(1–3), 169–192, doi:10.1016/0016-7061(90)90014-Z.

Castiglione, P., B. P. Mohanty, P. J. Shouse, J. Simunek, M. T. van Genuchten, and A. Santini (2003), Lateral water diffusion in an artificial macroporous system: Modeling and experimental evidence, *Vadose Zone J.*, *2*, 212–221.

Chen, C., and R. J. Wagenet (1992), Simulation of water and chemicals in macropore soils. Part 1. Representation of the equivalent macropore influence and its effect on soil water flow, *J. Hydrol.*, *130*, 105–126, doi:10.1016/0022-1694(92)90106-6.

Clausnitzer, V., and J. W. Hopmans (1995), Non-linear parameter estimation: LM_OPT, General-purpose optimization code based on the Levenberg-Marquardt algorithm, *Land Air Water Resour. Pap. 100032*, Univ. of Calif., Davis.

Das Gupta, S., B. P. Mohanty, and J. M. Köhne (2006), Soil hydraulic conductivities and their spatial and temporal variations in a Vertisol, *Soil Sci. Soc. Am. J.*, *70*, 1872–1881, doi:10.2136/sssaj2006.0201.

Dousset, S., M. Thevenot, V. Pot, J. Šimůnek, and F. Andreux (2007), Evaluating equilibrium and non-equilibrium transport of bromide and isoproturon in disturbed and undisturbed soil columns, *J. Contam. Hydrol.*, *94*, 261–276, doi:10.1016/j.jconhyd.2007.07.002.

Feyen, J., D. Jacques, A. Timmerman, and J. Vanderborght (1998), Modelling water flow and solute transport in heterogeneous soils: A review of recent approaches, *J. Agric. Eng. Res.*, *70*(3), 231–256, doi:10.1006/jaer.1998.0272.

Franzluebbers, A. J., F. M. Hons, and D. A. Zuberer (1995), Tillage-induced seasonal changes in soil physical properties affecting soil CO_2 evolution under intensive cropping, *Soil Tillage Res.*, *34*, 41–60, doi:10.1016/0167-1987(94)00450-S.

Freeze, R. A. (1975), A stochastic-conceptual analysis of one-dimensional groundwater flow in nonuniform homogeneous media, *Water Resour. Res.*, *11*, 725–741, doi:10.1029/WR011i005p00725.

Gee, G. W., C. T. Kincaid, R. J. Lenhard, and C. S. Simmons (1991), Recent studies of flow and transport in the vadose zone, *Rev. Geophys.*, *29*, 227–239.

Gerke, H. H. (2006), Preferential flow descriptions for structured soils, *J. Plant Nutr. Soil Sci.*, *169*(3), 382–400, doi:10.1002/jpln.200521955.

Gerke, H. H., and J. M. Köhne (2004), Dual-permeability modeling of preferential bromide leaching from a tile-drained glacial till agricultural field, *J. Hydrol.*, *289*, 239–257, doi:10.1016/j.jhydrol.2003.11.019.

Gerke, H. H., and M. T. van Genuchten (1993), A dual-porosity model for simulating the preferential movement of water and solutes in structured porous media, *Water Resour. Res.*, *29*, 305–319, doi:10.1029/92WR02339.

Gerke, H. H., and M. T. van Genuchten (1996), Macroscopic representation of structural geometry for simulating water and solute mass transfer in dual-porosity media, *Adv. Water Resour.*, *19*, 343–357, doi:10.1016/0309-1708(96)00012-7.

Germann, P. F. (1985), Kinematic wave approach to infiltration and drainage into and from soil macropores, *Trans. ASAE*, *28*(3), 745–749.

Hendrickx, J. M. H., and M. Flury (2001), Conceptual models of flow and transport in the fractured vadose zone, in *Uniform and Preferential Flow Mechanisms in the Vadose Zone*, pp. 149–187, Natl. Acad. Press, Washington, D. C.

Jamieson, R. C., R. J. Gordon, K. E. Sharples, G. W. Stratton, and A. Madani (2002), Movement and persistence of fecal bacteria in agricultural soils and subsurface drainage water—A review, *Can. Biosyst. Eng.*, *44*, 1.1–1.9.

Jansson, C., B. Espeby, and P.-E. Jansson (2005), Preferential water flow in a glacial till soil, *Nord. Hydrol.*, *36*, 1–11.

Jarvis, N. J. (1994), The MACRO model (version 3.1)—Technical description and sample simulation, *Rep. Diss. 10*, 51 pp., Dep. of Soil Sci., Swed. Univ. of Agric. Sci., Uppsala, Sweden.

Jarvis, N. J. (2007), A review of non-equilibrium water flow and solute transport in soil macropores: Principles, controlling factors and consequences for water quality, *Eur. J. Soil Sci.*, *58*, 523–546, doi:10.1111/j.1365-2389.2007.00915.x.

Jury, W. A., and H. Flühler (1992), Transport of chemicals through soil: Mechanisms, models and field applications, *Adv. Agron.*, *47*, 141–201, doi:10.1016/S0065-2113(08)60490-3.

Kladivko, E. J., L. C. Brown, and J. L. Baker (2001), Pesticide transport to subsurface tile drains in humid regions of North America, *Crit. Rev. Environ. Sci. Technol.*, *31*, 1–62, doi:10.1080/20016491089163.

Kodešová, R., M. Kočárek, V. Kodeš, J. Šimůnek, and J. Kozák (2008), Impact of soil micromorphological features on water flow and herbicide transport in soils, *Vadose Zone J.*, *7*, 798–809, doi:10.2136/vzj2007.0079.

Köhne, J. M., and B. P. Mohanty (2005), Water flow processes in a soil column with a cylindrical macropore: Experiment and hierarchical modeling, *Water Resour. Res.*, *41*, W03010, doi:10.1029/2004WR003303.

Köhne, J. M., S. Köhne, and H. H. Gerke (2002), Estimating the hydraulic functions of dual-permeability models from bulk soil data, *Water Resour. Res.*, *38*(7), 1121, doi:10.1029/2001WR000492.

Köhne, J. M., B. P. Mohanty, J. Šimůnek, and H. H. Gerke (2004), Numerical evaluation of a second-order water transfer term for variably saturated dual-permeability models, *Water Resour. Res.*, *40*, W07409, doi:10.1029/2004WR003285.

Köhne, J. M., S. Köhne, and J. Šimůnek (2006a), Multi-process herbicide transport in structured soil columns: Experiments and model analysis, *J. Contam. Hydrol.*, *85*, 1–32, doi:10.1016/j.jconhyd.2006.01.001.

Köhne, S., B. Lennartz, J. M. Köhne, and J. Šimůnek (2006b), Bromide transport at a tile-drained field site: Experiment, and one- and two-dimensional equilibrium and non-equilibrium numerical modeling, *J. Hydrol.*, *321*, 390–408, doi:10.1016/j.jhydrol.2005.08.010.

Köhne, J. M., S. Köhne, and J. Šimůnek (2009), A review of model applications for structured soils: a) Water flow and solute transport, *J. Contam. Hydrol.*, *104*, 4–35, doi:10.1016/j.jconhyd.2008.10.002.

Kramers, G., J. C. van Dam, C. J. Ritsema, F. Stagnitti, K. Oostindie, and L. W. Dekker (2005), A new modelling approach to simulate preferential flow and transport in water repellent porous media: Parameter sensitivity, and effects on crop growth and solute leaching, *Aust. J. Soil Res.*, *43*, 371–382, doi:10.1071/SR04098.

Larsson, M. H., N. J. Jarvis, G. Torstensson, and R. Kasteel (1999), Quantifying the impact of preferential flow on solute transport to tile drains in a sandy field soil, *J. Hydrol.*, *215*, 116–134, doi:10.1016/S0022-1694(98)00265-0.

Legates, D. R., and G. J. McCabe Jr. (1999), Evaluating the use of "goodness-of-fit" measures in hydrologic and hydroclimatic model validation, *Water Resour. Res.*, *35*, 233–241, doi:10.1029/1998WR900018.

Liu, K. H., C. G. Enfield, and S. C. Mravik (1991), Evaluation of sorption models in the simulation of naphthalene transport through saturated soils, *Ground Water*, *29*(5), 685–692, doi:10.1111/j.1745-6584.1991.tb00560.x.

Logsdon, S. D., and D. B. Jaynes (1996), Spatial variability of hydraulic conductivity in a cultivated field at different times, *Soil Sci. Soc. Am. J.*, *60*, 703–709, doi:10.2136/sssaj1996.03615995006000030003x.

Miller, J. J., B. J. Lamond, N. J. Sweetland, and F. J. Larney (1999), Preferential leaching in large undisturbed soil blocks from conventional tillage and no-till fields in southern Alberta, *Water Qual. Res. J. Can.*, *34*(2), 249–266.

Mualem, Y. (1976), A new model for predicting the hydraulic conductivity of unsaturated soils, *Water Resour. Res.*, *12*, 513–522, doi:10.1029/WR012i003p00513.

National Research Council (1994), *Ground Water Recharge Using Waters of Impaired Quality*, 283 pp., Natl. Acad. Press, Washington, D. C.

Novák, V., J. Šimůnek, and M. T. van Genuchten (2000), Infiltration of water into soils with cracks, *J. Irrig. Drain. Eng.*, *126*(1), 41–47, doi:10.1061/(ASCE)0733-9437(2000)126:1(41).

Schäffer, B., M. Stauber, T. L. Mueller, R. Müller, and R. Schulin (2008), Soil and macro-pores under uniaxial compression. I. Mechanical stability of repacked soil and deformation of different types of macro-pores, *Geoderma*, *146*(1–2), 183–191, doi:10.1016/j.geoderma.2008.05.019.

Schoups, G., and J. A. Vrugt (2010), A formal likelihood function for parameter and predictive inference of hydrologic models with correlated, heteroscedastic, and non-Gaussian errors, *Water Resour. Res.*, *46*, W10531, doi:10.1029/2009WR008933.

Šimůnek, J., M. Šejna, and M. T. van Genuchten (1998), The HYDRUS-1D software package for simulating the one-dimensional movement of water, heat, and multiple solutes in variably saturated media (version 2.0), *Rep. IGWMC-TPS-70*, 202 pp., Int. Ground Water Model. Cent., Colo. Sch. of Mines, Golden.

Šimůnek, J., O. Wendroth, and M. T. van Genuchten (1999), Estimating unsaturated soil hydraulic properties from laboratory tension disc infiltrometer experiments, *Water Resour. Res.*, *35*, 2965–2979, doi:10.1029/1999WR900179.

Šimůnek, J., O. Wendroth, N. Wypler, and M. T. van Genuchten (2001), Non-equilibrium water flow characterized by means of upward infiltration experiments, *Eur. J. Soil Sci.*, *52*(1), 13–24, doi:10.1046/j.1365-2389.2001.00361.x.

Šimůnek, J., N. J. Jarvis, M. T. van Genuchten, and A. Gärdenäs (2003), Review and comparison of models for describing non-equilibrium and preferential flow and transport in the vadose zone, *J. Hydrol.*, *272*, 14–35, doi:10.1016/S0022-1694(02)00252-4.

van Genuchten, M. T. (1980), A closed-form equation for predicting the hydraulic conductivity of unsaturated soils, *Soil Sci. Soc. Am. J.*, *44*, 892–898, doi:10.2136/sssaj1980.03615995004400050002x.

van Genuchten, M. T., and P. J. Wierenga (1976), Mass transfer studies in sorbing porous media I. Analytical solutions, *Soil Sci. Soc. Am. J.*, *40*, 473–481, doi:10.2136/sssaj1976.03615995004000040011x.

van Genuchten, M. T., D. E. Rolston, and P. F. Germann (1990), Transport of water and solutes in macropores, *Geoderma*, *46*(1), 1–297.

Villholth, K. G., and K. H. Jensen (1998), Flow and transport processes in a macroporous subsurface drained glacial till soil. II. Model analysis, *J. Hydrol.*, *207*, 121–135, doi:10.1016/S0022-1694(98)00130-9.

Vogel, T., H. H. Gerke, R. Zhang, and M. T. van Genuchten (2000), Modeling flow and transport in a two-dimensional dual-permeability system with spatially variable hydraulic properties, *J. Hydrol.*, *238*, 78–89, doi:10.1016/S0022-1694(00)00327-9.

Vrugt, J. A., W. Bouten, H. V. Gupta, and J. W. Hopmans (2003), Toward improved identifiability of soil hydraulic parameters: On the selection of a suitable parametric model, *Vadose Zone J.*, *2*, 98–113, doi:10.2113/2.1.98.

Weiler, M. (2005), An infiltration model based on flow variability in macropores: Development, sensitivity analysis and applications, *J. Hydrol.*, *310*, 294–315, doi:10.1016/j.jhydrol.2005.01.010.

Wu, C.-M., T.-C. J. Yeh, J. Zhu, T. H. Lee, N.-S. Hsu, C.-H. Chen, and A. F. Sancho (2005), Traditional analysis of aquifer tests: Comparing apples to oranges?, *Water Resour. Res.*, *41*, W09402, doi:10.1029/2004WR003717.

Yeh, T.-C. J., M. Ye, and R. Khaleel (2005), Estimation of effective unsaturated conductivity tensor using spatial moments of observed moisture plume, *Water Resour. Res.*, *41*, W03014, doi:10.1029/2004WR003736.

Zhang, K., Y. S. Wu, and J. Houseworth (2006), Sensitivity analysis of hydrological parameters in modeling flow and transport in the unsaturated zone of Yucca Mountain, Nevada, USA, *Hydrogeol. J.*, *14*(8), 1599–1619, doi:10.1007/s10040-006-0055-y.

Zurmühl, T., and W. Durner (1998), Determination of parameters for bimodal hydraulic functions by inverse modeling, *Soil Sci. Soc. Am. J.*, *62*, 874–880, doi:10.2136/sssaj1998.03615995006200040004x.

B. Arora and B. P. Mohanty, Department of Biological and Agricultural Engineering, Texas A&M University, College Station, TX 77843-2117, USA. (bmohanty@tamu.edu)

J. T. McGuire, Department of Geology and Geophysics, University of St. Thomas, St. Paul, MN 55105, USA.